

Solid-State NMR Determination of Peptide Torsion Angles: Applications of ^2H -Dephased REDOR

Ingolf Sack,[†] Yael S. Balazs,[†] Shai Rahimipour,[‡] and Shimon Vega^{*†}

Contribution from the Departments of Chemical Physics and Organic Chemistry, Weizmann Institute of Science, Rehovot 76100, Israel

Received February 8, 2000. Revised Manuscript Received September 25, 2000

Abstract: The backbone conformation of peptides and proteins is completely defined by the torsion angles (ϕ, ψ, ω) of each amino acid residue along the polypeptide chain. We demonstrate a solid-state NMR method based on heteronuclear distance measurements for determining (ϕ, ψ) angles. Simple and reliable deuterium phase modulated pulses (PM5) reintroduce dipolar couplings between ^2H and a spin- $1/2$ nucleus. Measuring the $^{13}\text{C}_{i-1}\{^2\text{H}_i^\alpha\}$ REDOR distance across a peptide bond results in the torsion angle ϕ_i as a consequence of the restricted geometry of the peptide backbone. The $^{15}\text{N}_{i+1}\{^2\text{H}_i^\alpha\}$ REDOR distance across a peptide bond defines the torsion angle ψ_i . This approach is demonstrated for both the 3-spin $\text{X}\{^2\text{H}_2\}$ REDOR case of glycine and the 2-spin $\text{X}\{^2\text{H}\}$ REDOR case, represented by L-alanine, using two different tripeptides. It is shown that the technique can handle multiple sample conformations. PM5-REDOR decay curves of the ψ angle show distinctly different behaviors between α -helix and β -sheet backbone conformations.

Introduction

The rapid rate at which high-resolution 3D protein structures are being solved is dramatic. The more than 13 000 structures of the Protein Data Bank (Research Collaboratory for Structural Bioinformatics, <http://www.rcsb.org/pdb>) attests to the success of protein structure determination in the crystalline state by X-ray crystallography and in solution by liquid-state nuclear magnetic resonance (NMR). Recent advances in both techniques suggest that the number of known structures will continue to escalate (see recent reviews, refs 1–4). Solid-state NMR provides a complementary high-resolution spectroscopic technique to determine local protein structure in disordered and anisotropic environments (reviews, refs 5–10). Routine high-resolution biomolecular structure determination of solids lacking long-range order may be feasible using solid-state NMR.^{11–15}

Solid-state NMR spectra contain information on anisotropic interactions (chemical shift, dipolar couplings, and quadrupolar couplings). Manipulation of the overabundance of information is necessary to obtain sufficient resolution to interpret the spectra. Of particular interest to protein structural studies have been methods measuring molecular orientations, internuclear distances, and the (ϕ, ψ) conformational angles.⁵ The 3D conformations of proteins are defined by the individual makeup of ϕ_i ($\text{C}_{i-1}\text{N}_i\text{C}_i^\alpha\text{C}_i$) and ψ_i ($\text{N}_i\text{C}_i^\alpha\text{C}_i\text{N}_{i+1}$) torsion angles of each amino acid residue along the polypeptide chain. Accurate knowledge of torsion angles is the basis of well-defined protein secondary structures. A number of techniques for determining peptide torsion angles using solid-state NMR were recently developed.^{12,16–26} The combination of multiple and highly

* To whom correspondence should be addressed.

[†] Department of Chemical Physics.

[‡] Department of Organic Chemistry.

(1) Beauchamp, J. C.; Isaacs, N. W. *Curr. Op. Chem. Biol.* **1999**, *3*, 525–529.

(2) Lindley, P. F. *Acta Crystallogr.* **1999**, D55, 1654–1662.

(3) Wider, G.; Wuthrich, K. *Curr. Op. Struct. Biol.* **1999**, *9*, 594–601.

(4) Siegal, G.; van Duynhoven, J.; Baldus, M. *Curr. Op. Chem. Biol.* **1999**, *3*, 530–536.

(5) Fu, R. Q.; Cross, T. A. *Annu. Rev. Biophys. Biomol. Struct.* **1999**, *28*, 235–268.

(6) Bechinger, B.; Kinder, R.; Helmle, H.; Vogt, T. C. B.; Harzer, U.; Schinzel, S. *Biopolymers* **1999**, *51*, 174–190.

(7) Garbow, J. R.; Gullion, T. *Measurement of internuclear distances in biological solids by magic-angle spinning ^{13}C NMR*; Beckman, N., Ed.; Academic Press: San Deigo, 1995; pp 65–115.

(8) Griffin, R. G. *Nature Struct. Biol.* **1998**, *5*, 508–512.

(9) Wemmer, D. *Methods Enzymol.* **1999**, *309*, 536–559.

(10) Davis, J. H.; Auger, M. *Prog. Nucl. Magn. Reson. Spectrosc.* **1999**, *35*, 1–84.

(11) Opella, S. J.; Marassi, F. M.; Gesell, J. J.; Valente, A. P.; Kim, Y.; Oblatt-Montal, M.; Montal, M. *Nature Struct. Biol.* **1999**, *6*, 374–379.

(12) Hong, M. *J. Magn. Reson.* **1999**, *139*, 389–401.

(13) Ketchum, R. R.; Roux, B.; Cross, T. A. *Structure* **1997**, *5*, 1655–1669.

(14) Marassi, F. M.; Ramamoorthy, A.; Opella, S. J. *Proc. Natl. Acad. Sci. U.S.A.* **1997**, *94*, 8551–8556.

(15) Sun, B.-Q.; Rienstra, C. M.; Costa, P. R.; Williamson, J. R.; Griffin, R. G. *J. Am. Chem. Soc.* **1997**, *119*, 8540–8546.

(16) Bower, P. V.; Oyler, N.; Mehta, M. A.; Long, J. R.; Stayton, P. S.; Drobny, G. P. *J. Am. Chem. Soc.* **1999**, *121*, 8373–8375.

(17) Nomura, K.; Takegoshi, K.; Terao, T.; Uchida, K.; Kainosho, M. *J. Am. Chem. Soc.* **1999**, *121*, 4064–4065.

(18) Ishii, Y.; Hirao, K.; Terao, T.; Terauchi, T.; Oba, M.; Nishiyama, K.; Kainosho, M. *Solid State Nucl. Magn. Reson.* **1998**, *11*, 169–175.

(19) Bennett, A. E.; Weliky, D. P.; Tycko, R. *J. Am. Chem. Soc.* **1998**, *120*, 4897–4898.

(20) Costa, P. R.; Gross, J. D.; Hong, M.; Griffin, R. G. *Chem. Phys. Lett.* **1997**, *280*, 95–103.

(21) Hong, M.; Gross, J. D.; Griffin, R. G. *J. Phys. Chem. B* **1997**, *101*, 5869–5874.

(22) Feng, X.; Eden, M.; Brinkmann, A.; Luthman, H.; Eriksson, L.; Graslund, A.; Antzutkin, O. N.; Levitt, M. H. *J. Am. Chem. Soc.* **1997**, *119*, 12006–12007.

(23) Heller, J.; Laws, D. D.; Tomaselli, M.; King, D. S.; Wemmer, D. E.; Pines, A.; Havlin, R. H.; Oldfield, E. *J. Am. Chem. Soc.* **1997**, *119*, 7827–7831.

(24) Tycko, R.; Weliky, D. P.; Berger, A. E. *J. Chem. Phys.* **1996**, *105*, 7915–7930.

(25) Schmidt-Rohr, K. *Macromolecules* **1996**, *29*, 3975–3981.

(26) Creuzet, F.; McDermott, A.; Gebhard, R.; van der Hoef, K.; Spijker-Assink, M. B.; Herzfeld, J.; Lugtenburg, J.; Levitt, M. H.; Griffin, R. G. *Science* **1991**, *251*, 783–786.

accurate solid-state NMR distance constraint measurements coupled to advanced computer modeling has been used to assign total conformations of proteins at the molecular level.^{11,13,27} Solid-state NMR can provide molecular level answers to biological questions by the use of local torsion angle probes as has already been demonstrated on a number of real systems.^{26,28–34}

The application of spin- $1/2$ to ^2H REDOR measurements reported here extends the available methods for determining torsion angles from internuclear distances.^{16,17,24,26} Heteronuclear distance measurements between a spin- $1/2$ nucleus (X) and a spin-1 deuterium (^2H) can be achieved during magic angle spinning (MAS) by reintroducing dipolar couplings using a variation of Rotational Echo Double Resonance (REDOR).^{35–42} Use of deuterium phase modulated rf-pulses (PM5) to reintroduce X- ^2H dipolar interactions and determine internuclear distances was demonstrated for L-alanine-2- d_1 and ethyl malonic acid-4- d_2 .⁴¹ A simple and powerful scheme for determining peptide backbone torsion angles is to incorporate commercially available amino acids that contain a nonexchangeable deuterium atom bound to the α carbon (Figure 1). To determine the torsion angle ϕ_i the amino acid prior to the $^2\text{H}^\alpha$ labeled residue is enriched with ^{13}C at the carbonyl carbon. ^{13}C -observed, $\{^2\text{H}\}$ -dephased REDOR internuclear distance measurements from the carbonyl $^{13}\text{C}_{i-1}$ to $^2\text{H}_i^\alpha$ restrict the possible ϕ_i angles across the $\text{C}_{i-1}\text{N}_i\text{C}_i^\alpha\text{C}_i$ bond. To determine the torsion angle ψ_i the amino acid following the $^2\text{H}^\alpha$ labeled residue is ^{15}N enriched at the amide position. ^{15}N -observed, $\{^2\text{H}\}$ -dephased REDOR distance measurements from $^2\text{H}_i^\alpha$ to $^{15}\text{N}_{i+1}$ define the torsion angle ψ_i across the $\text{N}_i\text{C}_i^\alpha\text{C}_i\text{N}_{i+1}$ bond.

The above newly introduced use of X- ^2H distances and general labeling strategy for defining protein secondary structure via determination of ϕ and ψ angles is easy to implement. We demonstrate the simplicity and versatility of this approach on two different selectively labeled tripeptides L-[1- ^{13}C , ^{15}N]Leu-[2,2- $^2\text{H}_2$]Gly-[^{15}N]Ala (LGA) and L-[1- ^{13}C , ^{15}N]Leu-[2- ^2H]Ala-[^{15}N]Phe (LAF). Conformational angles (ϕ, ψ) were determined for two tripeptides, LGA and LAF. Unique angles were obtained with additional $^{13}\text{C}\{^{15}\text{N}\}$ REDOR measurement constraints and a (ϕ, ψ) plot of experimentally observed amino acid conforma-

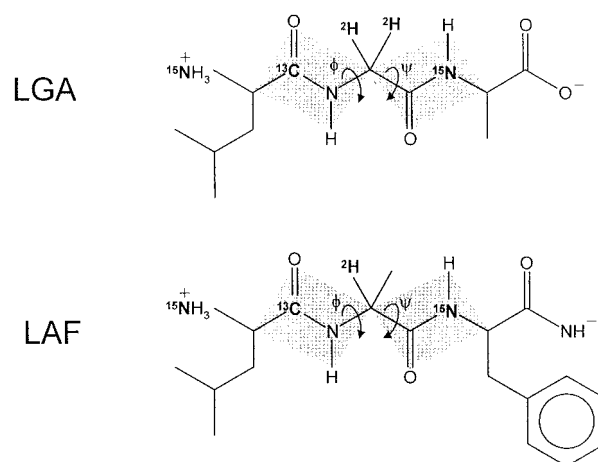


Figure 1. The sequences of the tripeptides investigated and the isotope labeling scheme used for determining the backbone torsion angles (ϕ, ψ). The torsion angles are shown with the conventional sense of rotation where looking along the backbone from the N-terminus, ϕ and ψ rotate in a positive clockwise sense, indicated by arrows.⁶⁰

tions.⁴³ The ability of ^2H -dephased REDOR torsion angle measurements to handle nonideal samples is demonstrated in the case of LAF where two conformations are observed by ^{13}C CPMAS.

Experimental Section

Tripeptide Synthesis and Purification. All chemicals and reagents are of analytical grade. L-Alanine- ^{15}N , L-alanine-2- d_1 , glycine-2,2- d_2 , L-leucine-1- $^{13}\text{C}, ^{15}\text{N}$, and L-phenylalanine- ^{15}N were purchased from Cambridge Isotope Laboratories (Andover, USA). The free α -amino groups were protected with Fluorenylmethoxycarbonyl (Fmoc) employing Fmoc-Osu as described elsewhere.⁴⁴ HPLC was done on a Spectra-Physics SP-8800 liquid chromatography system equipped with an Applied Biosystems 757 variable wavelength absorbance detector. Lichorcart columns were used prepacked with Lichrospher 100 RP-18 (250 \times 4 mm; 5 μm) for analytical purposes or with Lichrosorb RP-18 (250 \times 10 mm; 7 μm) for semipreparative purification [Merck (Darmstadt, Germany)]. A linear gradient of 10–80% buffer B in A (A = water containing 0.1% trifluoroacetic acid (TFA), B = acetonitrile: water (75:25, v:v) containing 0.1% TFA) over 50 min was used.

The two tripeptides L-[1- $^{13}\text{C}, ^{15}\text{N}$]Leu-[2,2- $^2\text{H}_2$]Gly-[^{15}N]Ala (LGA) and L-[1- $^{13}\text{C}, ^{15}\text{N}$]Leu-[2- ^2H]Ala-[^{15}N]Phe (LAF) were synthesized manually using an Fmoc strategy⁴⁵ on a chlorotriptyl resin for LGA and Rink amide resin for LAF (Novabiochem, L aufelfingen, Switzerland). Coupling was carried out in *N,N*-dimethylformamide (DMF) using benzotriazole-1-yl-oxy-tris-pyrrolidino-phosphonium hexafluorophosphate (PyBOP) as the coupling agent and *N*-methyl morpholine (NMM) as the base. The resulting peptides were cleaved from the resin using 2 mL of TFA:H₂O:triethylsilane (95:2.5:2.5, v/v) for 1 h at room temperature. Crude peptides were precipitated with an equivalent mixture of ice-cold *tert*-butyl methyl ether and petroleum ether (10 mL). Purification of products (>90%) was achieved with semipreparative HPLC. The peptides gave expected results for [M + H]⁺ mass peaks and amino acid analysis following hydrolysis with 6 M HCl at 110 $^\circ\text{C}$ for 22 h. Purified peptides were lyophilized overnight. The powders were packed into 7-mm NMR rotors. Initially the CPMAS spectra for LAF had very broad line widths and the $^{13}\text{C}\{^2\text{H}\}$ PM5-REDOR decay leveled off at long evolution times.⁴⁶ After approximately three weeks the LAF line widths narrowed and $^{13}\text{C}\{^2\text{H}\}$ PM5-REDOR decay curves could be described by theoretical curves.

(43) Karplus, P. A. *Protein Sci.* **1996**, *5*, 1406–1420.

(44) Ten Kortenaar, P. B. W.; Van Dijk, B. G.; Peeters, J. M.; Raaben, B. J.; Adam, P. J. H. M.; Tesser, G. I. *Int. J. Peptide Protein Res.* **1986**, *27*, 398–400.

(45) Carpino, L. A.; Han, G. Y. *J. Org. Chem.* **1972**, *37*, 3404–3409.

(46) Sack, I.; Balazs, Y. S.; Rahimpour, S.; Vega, S. *J. Magn. Reson.* **1999**, *in press*.

(27) Ketchum, R. R.; Lee, K. C.; Huo, S.; Cross, T. A. *J. Biomol. NMR* **1996**, *8*, 1–14.

(28) Weliky, D. P.; Bennett, A. E.; Zvi, A.; Anglister, J.; Steinbach, P. J.; Tycko, R. *Nature Struct. Biol.* **1999**, *6*, 141–145.

(29) Long, H. W.; Tycko, R. *J. Am. Chem. Soc.* **1998**, *120*, 7039–7048.

(30) Costa, P. R.; Kocisko, D. A.; Sun, B. Q.; Lansbury, P. T.; Griffin, R. G. *J. Am. Chem. Soc.* **1997**, *119*, 10487–10493.

(31) Feng, X.; Verdegem, P. J. E.; Lee, Y. K.; Sandstrom, D.; Eden, M.; Bovee-Geurts, P.; deGrip, W. J.; Lugtenburg, J.; deGroot, H. J. M.; Levitt, M. H. *J. Am. Chem. Soc.* **1997**, *119*, 6853–6857.

(32) Middleton, D. A.; Robins, R.; Feng, X. L.; Levitt, M. H.; Spiers, I. D.; Schwalbe, C. H.; Reid, D. G.; Watts, A. *FEBS Lett.* **1997**, *410*, 269–274.

(33) McDermott, A. E.; Creuzet, F.; Gebhard, R.; van der Hoef, K.; Levitt, M. H.; Herzfeld, J.; Lugtenburg, J.; Griffin, R. G. *Biochemistry* **1994**, *33*, 6129–6136.

(34) Tomita, Y.; O'Connor, E. J.; McDermott, A. *J. Am. Chem. Soc.* **1994**, *116*, 8766–8771.

(35) Gullion, T.; Schaefer, J. *J. Magn. Reson.* **1989**, *81*, 196–200.

(36) Schmidt, A.; Kowalewski, T.; Schaefer, J. *Macromolecules* **1993**, *26*, 1729–1733.

(37) Gullion, T. *Chem. Phys. Lett.* **1995**, *246*, 325–330.

(38) Sandstrom, D.; Hong, M.; Schmidt-Rohr, K. *Chem. Phys. Lett.* **1999**, *300*, 213–220.

(39) Sack, I.; Goldbourt, A.; Vega, S.; Buntkowsky, G. *J. Magn. Reson.* **1999**, *138*, 54–65.

(40) Gullion, T. *J. Magn. Reson.* **1999**, *139*, 402–407.

(41) Sack, I.; Vega, S. *J. Magn. Reson.* **2000**, *145*, 52–61.

(42) Kesling, B.; Hughes, E.; Gullion, T. *Solid State Nucl. Magn. Reson.* **2000**, *16*, 1–7.

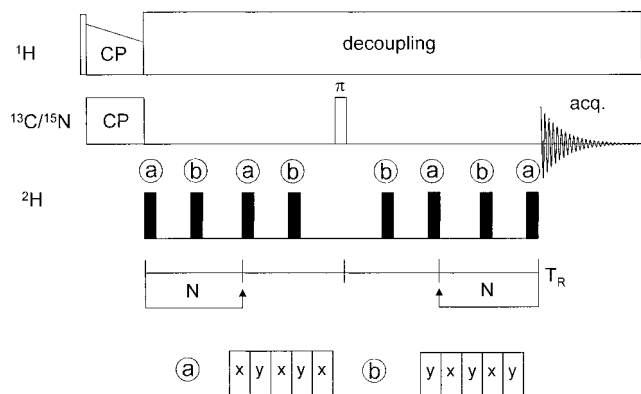


Figure 2. The $X\{^2\text{H}\}$ REDOR pulse sequence utilizing deuterium phase modulated pulses (PM5).⁴⁰

LGA: MS: found m/z $[\text{M} + \text{H}]^+$ 264.16, calculated for m/z $[\text{M} + \text{H}]^+$ 264.3. Amino acid analysis: Leu 0.92, Ala 1.01, Gly 1.06.

LAF: MS: found m/z $[\text{M} + \text{H}]^+$ 353.26, calculated m/z $[\text{M} + \text{H}]^+$ 353.22. Amino acid analysis: Leu 0.92, Ala 1.03, Phe 1.06

Solid-State NMR. REDOR experiments were performed on a Bruker DSX-300 spectrometer with resonance frequencies of 300.13 MHz for ^1H , 75.47 MHz for ^{13}C , 46.07 MHz for ^2H , and 30.41 MHz for ^{15}N . A standard Bruker 7-mm triple resonance HP probe with inserts for either $^{13}\text{C}/^2\text{H}$, $^{15}\text{N}/^2\text{H}$, or $^{13}\text{C}/^{15}\text{N}$ was used with zirconia rotors and 5 kHz sample spinning speeds. Cross-polarization (CP) with a ramped-amplitude⁴⁷ proton spin-locking field was used with a ramp changing from 100% to 50% maximum intensity within a 2 ms contact time. An independent proton power level was used for TPPM decoupling using a 65 kHz rf field. A single π pulse of 8 μs for ^{13}C or 16 μs for ^{15}N was applied on the observe channel to refocus the observed spins. For the reference REDOR experiment (S_0) no recoupling pulses were applied to the spin system on the third channel (^2H). ^{13}C chemical shifts were referenced to an external $^{13}\text{C}=\text{O}$ glycine sample at 176.04 ppm.²³ ^{15}N chemical shifts were referenced to an external $^{15}\text{NH}_4\text{Cl}$ (solid) sample at 38.5 ppm.⁴⁸

The $X\{^2\text{H}\}$ dipolar recoupling of the PM5-REDOR dephased spectra (S) was performed by applying two PM5 phase modulated pulses⁴¹ per rotor cycle in a mirror symmetric XY alternation (Figure 2). Unlike what occurs under multiple echo pulses on the observe channel, the signal decay during the dipolar evolution period in PM5-REDOR experiments is not influenced by pulse imperfections. This allows measurements of $^{13}\text{C}\{^2\text{H}\}$ or $^{15}\text{N}\{^2\text{H}\}$ dipolar dephasing over the long evolution periods (>25 ms) necessary to evaluate weak dipolar decays. Such weak dipolar dephasing is expected for $^2\text{H}-^{15}\text{N}$ spin pairs in peptide backbones where the range of possible ψ torsion angles corresponds to dipolar coupling strengths between 49 and 109 Hz.

The effect of the power level of the PM5 pulses on the observed REDOR dephasing for 2- and 3-spin models is simulated in Figure 3. The strongest effect of the PM5-recoupling pulses occurs at the minima of both curves, approximately 36 kHz. This demonstrates that optimal $^{13}\text{C}\{^2\text{H}\}$ and $^{15}\text{N}\{^2\text{H}\}$ dipolar recoupling is obtained with moderate rf-field strengths on the deuterium channel. With the deuterium pulse rf-power optimally set around 36 kHz, a PM5 pulse segment time of 5.6 μs is employed giving an overall pulse length of 28 μs . The ^2H pulse power for the $^{13}\text{C}\{^2\text{H}\}$ PM5-REDOR experiments was determined to be 32 kHz and for $^{15}\text{N}\{^2\text{H}\}$ PM5-REDOR 36 kHz. The different power levels result from the change in the triple tuned probe inserts and channels. Both the measured power levels are within the optimal range for deuterium dephasing with PM5 pulses. The experimental parameters for $^{13}\text{C}\{^2\text{H}\}$ REDOR were verified on alanine-2- d_1 resulting in good agreement with the crystal structure.⁴⁹ Alanine-2- d_1 is a good reference standard since its ^2H quadrupolar coupling strength is similar to that

(47) Metz, G.; Wu, X. L.; Smith, S. O. *J. Magn. Reson.* **1994**, *A110*, 219–227.

(48) McDermott, A.; Gu, Z. *Encyclopedia of Nuclear Magnetic Resonance*; Grant, D. A., Harris, R. K., Eds.; John Wiley and Sons: Chichester, 1996; Vol. 2, pp 1137–1147.

(49) Simpson, H. J.; Marsh, R. E. *Acta Crystallogr.* **1966**, *20*, 550.

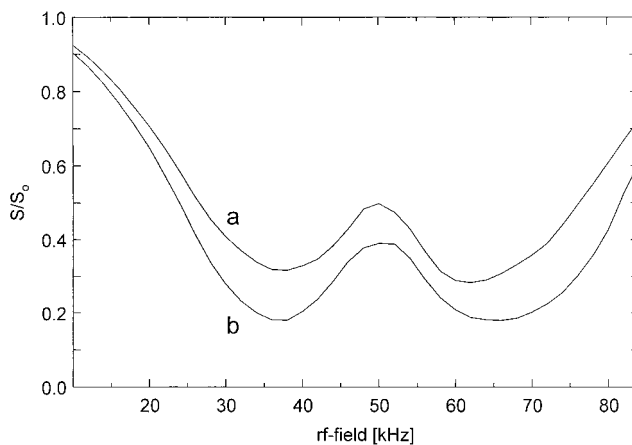


Figure 3. The calculated dependence of $^{13}\text{C}\{^2\text{H}\}$ PM5-REDOR dephasing after 10 ms evolution time on the deuterium rf irradiation intensities for a 2-spin $^{13}\text{C}\{^2\text{H}\}$ model where $\phi = +45^\circ$ (a) and a 3-spin $^{13}\text{C}\{^2\text{H}_2\}$ model where $\phi = +50^\circ$ (b).

found for a $^2\text{H}^{\alpha}$ -labeled polypeptide. A similar reference experiment for $^{15}\text{N}\{^2\text{H}\}$ is recommended using a deuterium standard with ^{15}N enrichment.³⁹

The deuterium rf power level was measured with a nutation experiment over a 360° rotation observing the behavior of the center band plus 5 pairs of spinning sidebands at 5 kHz magic-angle spinning. The rf irradiation intensity for the deuterium channel was calculated as the inverse of the pulse length at 360° . Knowledge of the experimental deuterium rf power to within ± 2 kHz is sufficient to simulate REDOR dephasing curves.⁴¹ Another input parameter for the REDOR decay curve simulations is the quadrupolar coupling strength. This was measured by detecting ^2H MAS spectra at 2 and 3 kHz spinning speeds and simulating the spinning sideband patterns to determine the deuterium quadrupolar coupling strength. The fid's of the MAS spectra were left shifted to begin at the second rotational echo before Fourier transformation. LGA, LAF, and the model compound alanine-2- d_1 all had quadrupolar coupling strengths of $125(\pm 3)$ kHz.

Numerical Simulations. $X\text{-}^2\text{H}$ REDOR decay curve simulations are straightforward calculations based on a stepwise integration of the Liouville–von Neumann density matrix equation⁴¹ with a program written in Matlab (The MathWorks, Inc., Natick, MA). The 2-spin case employed powder integration with 1154 sets of Euler triplets while 537 sets of Euler triplets were used in the 3-spin case of glycine.⁵⁰ The simulations implement the entire mirror symmetric pulse sequence for the ^2H excitation profile and take approximately 15 min for a 2-spin system or 30 min for a 3-spin system on a pentium III 400 MHz computer.

Experimental parameters used in the simulations are the PM5 pulse length and rf irradiation intensity, the spinning speed, and the magnitude of the ^2H quadrupolar coupling. The simulations assume the peptide bond is planar and that the torsion angle around the peptide bond is fixed. Figure 4 gives the standard bond distances and angles (Insight II, Molecular Simulations Inc., San Diego, CA) used to make the model. It is assumed that the ^2H quadrupolar tensor is aligned with and fixed to the direction of the $^2\text{H}_i\text{-C}_i^\alpha$ bond. The only free parameter is the ϕ or ψ torsion angle. In this model the dipolar interaction strength and the dipolar tensor are calculated as a function of the torsion angle. For any given torsion angle the determined dipolar interaction and dipolar tensor orientations are used to calculate a PM5-REDOR decay curve. Varying the torsion angle in steps of 18° generates a set of eleven PM5-REDOR decay curves between 0° and 180° . The theoretical curves are compared to the experimental decay curve. The angle determination is then refined by calculating curves with 5° torsion angle increments around the angle of interest. Several precalculated curves are available over the Internet at <http://userpage.chemie.fu-berlin.de/~sack/PM5REDOR/pm5redor.htm>.

(50) Conroy, H. *J. Chem. Phys.* **1967**, *47*, 5307.

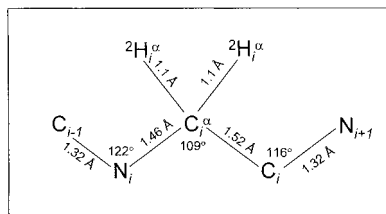


Figure 4. The indicated standard bond lengths and angles (Insight II, Molecular Simulations Inc., San Diego, CA) are fixed in the geometric model. The following assumptions are employed in the model: bond lengths and angles are independent of the torsion angle, the peptide plane is flat, and the quadrupolar tensor is aligned with the $^2\text{H}-\text{C}_i^\alpha$ bond. The only free parameter in $^{13}\text{C}\{^2\text{H}\}$ PM5-REDOR decay simulations is ϕ . The only free parameter in $^{15}\text{N}\{^2\text{H}\}$ PM5-REDOR decay simulations is ψ . For any given torsion angle the model is used to calculate the $^{13}\text{C}\{^2\text{H}\}$ or $^{15}\text{N}\{^2\text{H}\}$ dipolar coupling (internuclear distance) and its tensor orientation relative to the deuterium quadrupolar coupling (angle with the $^2\text{H}-\text{C}_i^\alpha$ bond). From these two parameters the PM5-REDOR decay curves are calculated. The tensor asymmetry is assumed to be zero.

The sensitivity of simulations to the model assumptions of Figure 4 was checked. All bond lengths were changed by ± 0.02 Å or all bond angles by $\pm 2^\circ$ from the standard model (Figure 4). This changed the torsion angle by $\pm 10^\circ$, calculated for an intermediate interaction strength ($\phi = 90^\circ$). Another model assumption inherent to the labeling scheme of Figure 1 is that spin- $1/2$ recoupling to deuterium is unaffected by the nonobserved spin- $1/2$. This was checked with a 3-spin simulation ($^{13}\text{C}/^1\text{H}/^{15}\text{N}$). The backbone $^{15}\text{N}-^2\text{H}$ distance was maximized (weakest interaction) and the $^{13}\text{C}-^2\text{H}$ distance minimized (strongest interaction). The influence of ^{13}C on the $^{15}\text{N}\{^2\text{H}\}$ PM5-REDOR decay was insignificant ($< 1\%$ at 25 ms). Perturbations to $^{13}\text{C}\{^2\text{H}\}$ recoupling by the presence of ^{15}N are even smaller.

Results

$^{15}\text{N}/^{13}\text{C}$ CP-MAS Spectra. The enriched terminal ^{15}N amino group and ^{15}N amide backbone (Figure 1) appear as two well-resolved peaks (Figure 5a,b). The broader (2 ppm) amide backbone resonance occurs at 124.4 ppm for LGA and at 119.1 ppm for LAF. The narrower (1 ppm) terminal $^{15}\text{NH}_2$ resonance occurs at 43.1 ppm for LGA and at 42.3 ppm for LAF. The single enriched ^{13}C label at the leucine carbonyl carbon results in one peak with an isotropic chemical shift of 171.8 ppm and a line width of 1 ppm for the LGA peptide (Figure 5c). The LAF peptide contains two isotropic chemical shifts for the single ^{13}C label (Figure 5d). The chemical shifts occur at 170.7 (peak A) and 170.0 ppm (peak B) with similar line widths of approximately 0.7 ppm. The splitting of the leucine carbonyl resonance into two lines separated by 0.7 ppm attests to conformational disorder in the sample and affects the evaluation of $^{13}\text{C}\{^2\text{H}\}$ REDOR experiments.

The principal CSA tensor values σ_{11} , σ_{22} , and σ_{33} were determined by Herzfeld–Berger analysis⁵¹ of the spinning sidebands at 2 kHz. It is interesting to note that the σ_{22} values shift slightly toward higher fields in the order LGA, LAF(A), LAF(B). The magnitude of the σ_{22} tensor does not appear to indicate a significant difference between hydrogen bonding environments of the backbone carbonyl of alanine.^{52,53} All ^{13}C CSA tensor values and asymmetry parameters are summarized in Table 1.

$^{13}\text{C}\{^2\text{H}\}$ REDOR Experiments. The measured T_2 decay of the leucine carbonyl is 10.5 ms. Within 6.2 ms the REDOR

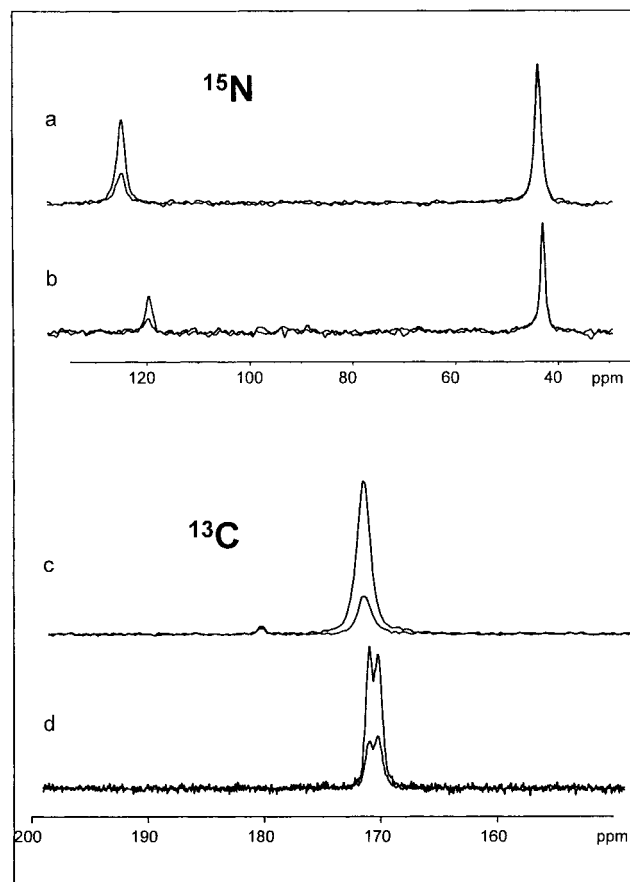


Figure 5. Reference and dephased LGA (a, c) and LAF (b, d) spectra after 10 ms (^{13}C) and 14.8 ms (^{15}N) evolution time. (d) The 170.7 ppm peak (A) and the 170.0 ppm peak (B) are both due to the single ^{13}C -enriched site of leucine in the LAF peptide. Fifty transients (LGA) and 100 transients (LAF) are used for both ^{13}C and ^{15}N observation.

Table 1. Leucine Carbonyl Carbon Chemical Shift Anisotropy Tensors and Asymmetry Comparisons between the Three Tripeptides^a

	σ_{iso} (ppm)	$\sigma_{\text{iso}} - \sigma_{11}$ (ppm)	$\sigma_{\text{iso}} - \sigma_{22}$ (ppm)	$\sigma_{\text{iso}} - \sigma_{33}$ (ppm)	η^b
LGA	171.8	76.8	-6.6	-70.2	0.83
LAF(A)	170.7	88.8	-2.6	-86.1	0.94
LAF(B)	170.0	73.6	0.7	-74.2	0.98

^a No significant differences in H-bonding environments of the alanine backbone carbonyl between the two LAF peaks is concluded based on the σ_{22} values.⁵³ ^b $|\sigma_{xx} - \sigma_{yy}|/|\sigma_{zz} - \sigma_{\text{iso}}|$.

signal dephased to half of its initial signal intensity. The experimental and simulated $^{13}\text{C}\{^2\text{H}\}$ REDOR decay curves of the LGA peptide are presented in Figure 6a. The experimental data are best represented by a simulation of $\phi = \pm 70^\circ$, shown as a bold line. An estimation of $\phi \pm 10^\circ$ on the torsion angle measurement is a result of bracketing the scatter in the data for dephasing times less than 15 ms. REDOR dephasing times longer than T_2 show significant decreases in signal-to-noise. This results in increased scatter of the data toward the end of the decay curve.

For the second peptide (LAF) the two resolved ^{13}C peaks have distinct REDOR decay curves (Figure 6c). The T_2 dephasing times of the two peaks were 14.5 ms for peak A and 12.0 ms for peak B. Each peak corresponds to a different conformation present in the LAF sample. The low field shifted signal (A) is best represented by the simulated curve corresponding to $\phi = +65^\circ$ or $\phi = +175^\circ$. The upfield LAF signal (B) yields $\phi = +50^\circ$ or $\phi = -170^\circ$. The error range for torsion

(51) Herzfeld, J.; Berger, A. E. *J. Chem. Phys.* **1980**, *73*, 6021–6030.

(52) Asakawa, N.; Kuroki, S.; Kurosu, H.; Ando, I.; Shoji, A.; Ozaki, T. *J. Am. Chem. Soc.* **1992**, *114*, 3261–3265.

(53) Gu, Z.; Zambrano, R.; McDermott, A. *J. Am. Chem. Soc.* **1994**, *116*, 6368–6372.

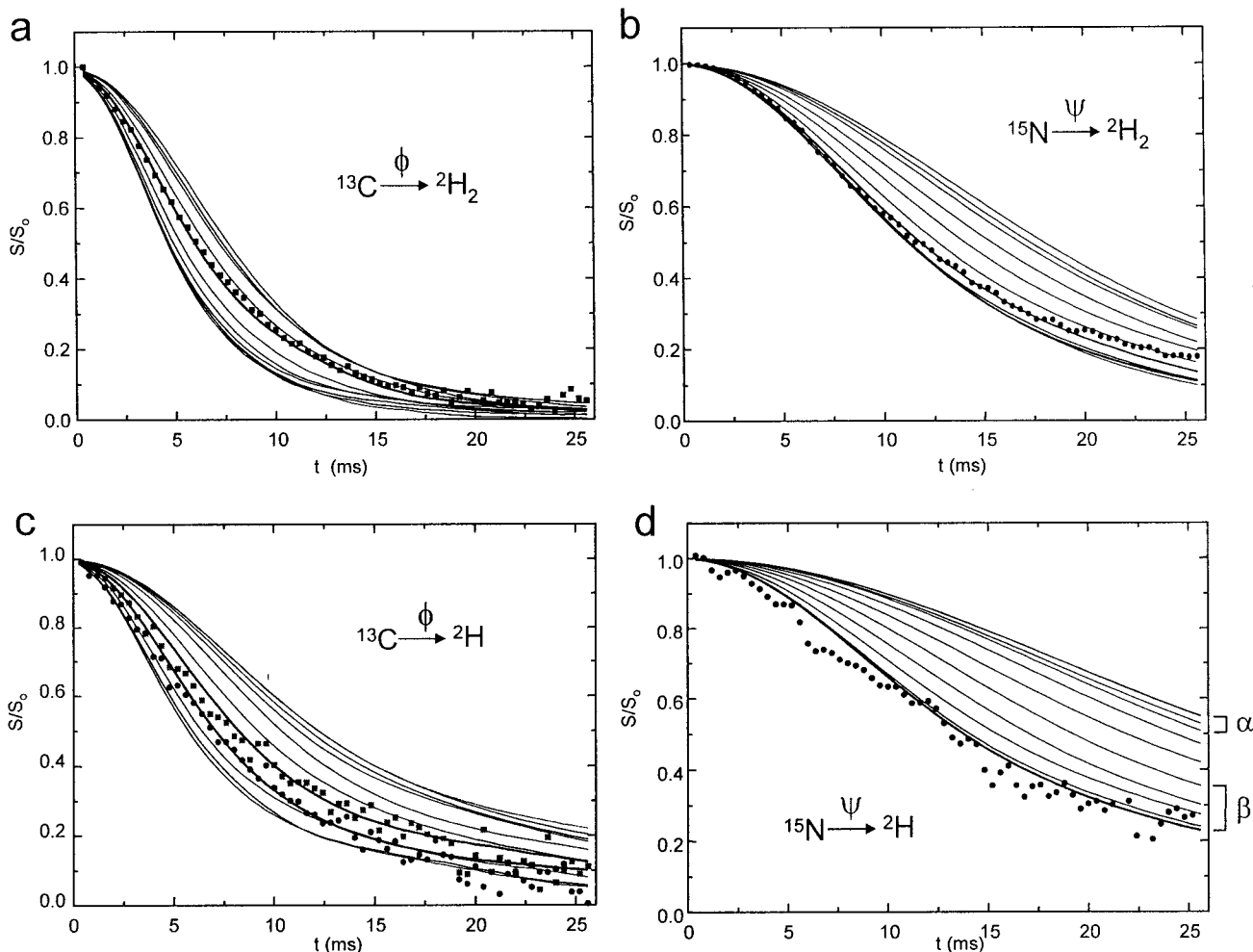


Figure 6. PM5-REDOR curves for 3-spin $X\{^2\text{H}_2^\alpha\}$ (a, b) and 2-spin $X\{^2\text{H}^\alpha\}$ cases (c, d). In the 3-spin case the upper curve represents a torsion angle of 0° and the lower curve $\pm 180^\circ$. For the nonglycine, 2-spin case, the upper curve represents a -60° torsion angle and the lower curve a $+120^\circ$ angle (see text). The angle ϕ is determined by $^{13}\text{C}\{^2\text{H}\}$ PM5-REDOR experiments (a, c). The angle ψ is determined by $^{15}\text{N}\{^2\text{H}\}$ PM5-REDOR experiments (b, d). The data for curves b and d were smoothed by adjacent averaging over five points. The faster decay curve in plot c is due to the 170.7 ppm LAF signal (A) and the upper decay curve is due to the 170.0 ppm LAF signal (B). Simulated values of ψ show good resolution between α -helix (upper curves) and β -sheet (lower curves) conformations.

angles $\phi(\text{A})$ and $\phi(\text{B})$ was estimated to be $\pm 15^\circ$ based on the scatter in the data for dephasing times less than 15 ms. At long evolution times the experimental REDOR dephasing for signal (A) shows a stronger decay than the calculated curves predict. Signal B has a slightly weaker decay within the range of the calculated curves, but shows the same overall behavior. The approximately 15° difference between the ^{13}C decay curves for the two conformations of LAF, (A) and (B), is constant for all dephasing times.

$^{15}\text{N}\{^2\text{H}\}$ REDOR Experiments. A single backbone ^{15}N CP-MAS signal is present for both LGA and LAF. ^{15}N -observed, $\{^2\text{H}\}$ -recoupled PM5-REDOR simulations and LGA and LAF experimental decay curves are shown in Figure 6b,d. The experimental REDOR signal decays toward 20% of the initial intensity after 25 ms. Two possible torsion angles $\psi = \pm 105^\circ$ are consistent with the LGA data. The scatter in the data is estimated to be $\pm 10^\circ$ for evolution times less than 15 ms. The LAF data give an immediate qualitative conformational angle consistent with β -sheet (rather than α -helix) structures directly and distinctly from the REDOR plots. For all 2-spin plots of $^{15}\text{N}\{^2\text{H}\}$ REDOR decay the upper curves correspond to torsion angles found in α -helical backbone conformations and the lower curves are for β -sheet conformational angles. Quantitatively the LAF $^{15}\text{N}-^2\text{H}$ interaction is clearly represented by the strongest

possible decay. The strongest interaction occurs when the $^2\text{H}^\alpha$ and ^{15}N are eclipsed which in L-isomers occurs when $\psi = +120^\circ$. The high density of the REDOR decay curves in this region results in a relatively large uncertainty for ψ estimated from scatter in the data to be $\pm 20^\circ$.

$^{15}\text{N}\{^{13}\text{C}\}$ REDOR Experiments. A ^{15}N -observed, $\{^{13}\text{C}\}$ -dephased REDOR measurement in LGA between L-alanine- ^{15}N and L-leucine-1- $^{13}\text{C},^{15}\text{N}$ or in LAF between L-phenylalanine- ^{15}N and L-leucine-1- $^{13}\text{C},^{15}\text{N}$ provides an additional structural constraint readily obtained with the labeling scheme of Figure 1. A ^{13}C -observed REDOR experiment would not be practical in this case since the more strongly $^{15}\text{N}-^{13}\text{C}$ dipolar coupled pair would dominate the distance measurement; in the ^{15}N -observed experiment each ^{15}N site can be evaluated separately. The two-bond distant, terminal $^{15}\text{N}-^{13}\text{C}$ pair of leucine provides an internal distance standard expected to be $2.46(\pm 0.04)$ Å, an average distance from 10 peptide crystal structures (Cambridge Database). The measured $^{15}\text{N}-^{13}\text{C}$ REDOR dipolar coupling strengths were $182(\pm 10)$ Hz for the LGA peptide and $183(\pm 10)$ Hz for LAF. A 10% correction of the dipolar coupling was necessary to obtain an internuclear distance of $2.46(\pm 0.05)$ Å in agreement with the expected value.

The four-bond distant ^{13}C to ^{15}N pair in LGA results in a dipolar interaction strength of $38(\pm 5)$ Hz corresponding to

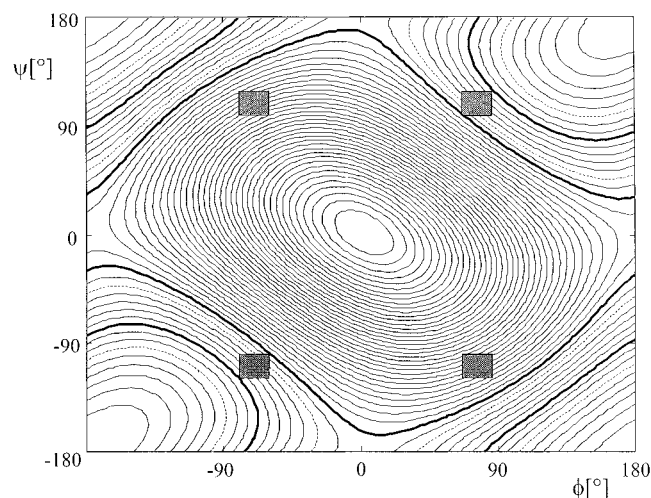


Figure 7. A Ramachandran contour plot of equidistant ^{15}N – ^{13}C internuclear distances spaced at 0.0525 Å. The LGA four-bond distant $^{15}\text{N}\{^{13}\text{C}\}$ REDOR measurement of 4.1 ± 0.2 Å is plotted as a bold line for the two extreme values. The uncorrected values for the $^{15}\text{N}\{^{13}\text{C}\}$ REDOR distance range are plotted as dotted lines. The gray patches represent four degenerate (ϕ, ψ) possibilities that fit the PM5-REDOR data for LGA: $\phi_{\text{Gly}} = \pm 70^\circ (\pm 10^\circ)$, $\psi_{\text{Gly}} = \pm 105^\circ (\pm 10^\circ)$. The $^{15}\text{N}\{^{13}\text{C}\}$ REDOR measurement constrains the torsion angles to be the same sign.

$4.3(\pm 0.2)$ Å. Applying the same 10% correction used on the reference measurement gives a distance of $4.1(\pm 0.2)$ Å. This correction is within the uncertainty of the measurements and the corrected and uncorrected values similarly constrain the measured LGA torsion angles of glycine to have the same sign (Figure 7). The LAF four-bond distant ^{13}C to ^{15}N pair measurement resulted in $32(\pm 10)$ Hz coupling.

(ϕ, ψ) Angle Constraints. A contour plot of the (ϕ, ψ) angles possible for a given ^{15}N – ^{13}C distance is plotted in Figure 7. The limits of the measured four-bond distant ^{15}N – ^{13}C pair for LGA are plotted as bold lines (the uncorrected distance is plotted as a dashed line). The experimental (ϕ, ψ) conformational angles and their error ranges are plotted as shaded gray patches. Overlap between the experimentally determined structural parameters clearly only occurs for (ϕ, ψ) angles of identical signs.

In the LAF peptide the $^{15}\text{N}\{^2\text{H}\}$ PM5-REDOR experiment uniquely determined the angle $\psi = +120^\circ$. A contour plot using the $^{13}\text{C}\{^{15}\text{N}\}$ REDOR distance to distinguish between possible ϕ values favors $\phi = +175^\circ$ and $\phi = -170^\circ$ but does not definitively rule out the possibility of $\phi = +65^\circ$ and $\phi = +50^\circ$ (data not shown). However, ϕ angles in the vicinity of $\pm 180^\circ$ are clearly preferred by referring to a Ramachandran plot of empirically observed amino acid conformations of nonglycine, nonproline residues.⁴³

Discussion

The conformational angles (ϕ, ψ) define the backbone geometry of proteins. Solid-state NMR is a powerful tool for determining (ϕ, ψ) in disordered and anisotropic environments. The straightforward strategy introduced here for determining peptide backbone conformations utilizes $^{13}\text{C}\{^2\text{H}\}$ REDOR to directly obtain the $\text{C}_{i-1}\text{N}_i\text{C}_i\text{C}_{i+1}$ torsion angle ϕ_i and $^{15}\text{N}\{^2\text{H}\}$ REDOR to determine the $\text{N}_i\text{C}_i\text{C}_{i+1}\text{N}_{i+1}$ torsion angle ψ_i . We used deuterium phase modulated pulses (PM5) and an XY-mirror symmetric pulse sequence to reintroduce X– ^2H dipolar couplings.^{39,41} In addition to the excellent accuracy of PM5-REDOR,⁴¹ the technique is easy to use. It requires the same equipment needed for standard spin- $1/2$ REDOR with the

addition of an appropriate ^2H –X insert for proper tuning of the three-channel probe. The modest power levels of the experiment are easily managed by a commercial spectrometer.

Analysis of the data is straightforward. To simulate REDOR decay curves the input parameters are well-defined. The only variable is the torsion angle. Given a torsion angle the model (Figure 4) calculates the corresponding X– ^2H internuclear distance and dipolar tensor orientation from which the PM5-REDOR curve is calculated. The 3-spin decay curves for the special case of glycine (Figures 6a,b) show the strongest decay (lower curve) when ϕ or $\psi = \pm 180^\circ$ and the weakest decay (upper curve) for ϕ or $\psi = 0^\circ$. The 3-spin case has a torsion angle defined as 180° when the Newman projection of the labeled X nucleus is precisely centered between the two ^2H 's. The opposite conformation corresponds to 0° .

For L-isomers (2-spin case), when the $^2\text{H}^\alpha$ is eclipsed with the labeled ^{13}C or ^{15}N the respective torsion angle ϕ or ψ is $+120^\circ$, whereas the trans conformation corresponds to a torsion angle of -60° . The strongest decay occurs when the isotopes are closest in the eclipsed conformation. Simulated decays (Figure 6c,d) vary from -60° (upper curve) to $+120^\circ$ (lower curve). Each remaining curve represents some intermediate backbone conformation of an L-amino acid and corresponds to two indistinguishable torsion angle values (ϕ, ϕ') which are related by $\phi' = 240^\circ - \phi$. The same holds true for (ψ, ψ') . To discriminate between the two values the labeling scheme in Figure 1 provides a natural four-bond distant $^{15}\text{N}\{^{13}\text{C}\}$ REDOR distance constraint. Another resource for further constraints of the backbone conformations is Ramachandran plots of theoretically allowed (ϕ, ψ) regions^{54,55} or experimentally observed regions from 70 diverse proteins.⁴³

Two different X– ^2H labeled tripeptides, LGA (3-spin system) and LAF (2-spin system), were synthesized to demonstrate the feasibility of the X $\{^2\text{H}\}$ REDOR method of torsion angle determination. The LGA sample contains a single CPMAS peak for each isotopically labeled nucleus (Figure 5c) and agreement with simulated REDOR decay curves is good (Figures 6a,b). The ^{13}C LAF spectrum shows two resolved peaks corresponding to two different conformations of the peptide (Figure 5d). There is a clear and constant REDOR decay difference of $\sim 15^\circ$ maintained between the data for each of the two conformations of LAF (Figure 6c). The presence of two LAF conformations did not interfere with the $^{13}\text{C}\{^2\text{H}\}$ PM5-REDOR determination of ϕ torsion angles for each signal. Experimental noise limits the certainty of the measurement to approximately $\pm 15^\circ$.

One nice feature of the curves is the clear discrimination between α -helix and β -sheet conformational angles⁵⁶ by ψ angle measurements. Chemical shift alone is also indicative of α -helix or β -sheet backbone conformations. The observed ^{13}C -Leu chemical shift is consistent with a β -sheet conformation.⁵⁷ Despite the large scatter in the $^{15}\text{N}\{^2\text{H}\}$ PM5-REDOR decay curve (Figure 6d) due to low signal-to-noise of the LAF amide backbone spectra (Figure 5b), it is still clear from the experimental curves that the structure agrees with a β -sheet. The modulation in the $^{15}\text{N}\{^2\text{H}\}$ PM5-REDOR decay curves (Figure 6 b,d) is observable in both the S and S_0 spectra (data not shown). We do not yet have an explanation for the source of this effect.

(54) Ramachandran, G. N.; Ramakrishnan, C.; Sasisekharan, V. *J. Mol. Biol.* **1963**, *7*, 95–99.

(55) Ramachandran, G. N.; Sasisekharan, V. *Adv. Protein Chem.* **1968**, *23*, 283–437.

(56) Mandel, N.; Mandel, G.; Trus, B. L.; Rosenberg, J.; Carlson, G.; Dickerson, R. E. *J. Biol. Chem.* **1977**, *252*, 4619–4636.

(57) Saito, H. *Magn. Reson. Chem.* **1986**, *24*, 835–852.

In general, experimental accuracy is affected by the density of the theoretical decay curves around the angle of interest. In all cases the calculated curves are most dense along the outermost regions making small angular differences difficult to discriminate. In the region where curves are spaced further apart the torsion angle values can be more finely determined. It has already been demonstrated that accurate quantitative values result from a good overall fit of the REDOR data with simulated curves for $^{13}\text{C}\{^2\text{H}\}$ PM5-REDOR experiments on two model compounds, L-alanine-2- d_1 and ethyl malonic acid-4- d_2 .⁴¹

The conformational angles (ϕ, ψ) are measured independently within a single sample using the labeling scheme in Figure 1. Commercially available nonexchangeable $^2\text{H}^\alpha$ labels can be incorporated into biomolecular samples using standard methods of peptide synthesis. Similarly, biosynthetic labeling of proteins using commercially available deuterated amino acids as starting materials can be supplemented into an appropriate growth media of choice depending on the overall labeling scheme desired.^{58,59} The multiple labeling used with this technique lends itself to maximizing the spectroscopic information available from a single sample. The signal-to-noise achievable with PM5-REDOR⁴¹ means that scaling up to larger biomolecular systems is quite feasible with this method.

This is a versatile technique offering a wide-range of possible applications. The use of a ^2H isotope lends itself to multi-labeling schemes that can combine targeted internuclear distance measurements between other isotopes. It can also be used with ^2H NMR studies for investigations of dynamics.⁴⁶ Applications include the targeting of conserved amino acids along a hinge or a bend to probe local conformations and dynamics, monitor-

ing changes in local secondary structure during thermal denaturation, or comparing changes in local structure between trapped intermediates. Resolution of multiply labeled samples could be achieved by extending this technique to higher dimensions.

Conclusion

Peptide backbone conformational angles (ϕ, ψ) are determined for the tripeptides shown in Figure 1. A $^{13}\text{C}\{^2\text{H}\}$ PM5-REDOR measurement of the peptide L-[1- ^{13}C , ^{15}N]Leu-[2,2- $^2\text{H}_2$]Gly-[^{15}N]Ala results in $\phi_{\text{Gly}} = \pm 70^\circ (\pm 10^\circ)$ and $^{15}\text{N}\{^2\text{H}\}$ PM5-REDOR gives $\psi_{\text{Gly}} = \pm 105^\circ (\pm 10^\circ)$. A Ramachandran contour plot of (ϕ, ψ) and a $^{13}\text{C}\{^{15}\text{N}\}$ REDOR distance constraint restrains ϕ_{Gly} and ψ_{Gly} to be the same sign. The second tripeptide L-[1- ^{13}C , ^{15}N]Leu-[2- ^2H]Ala-[^{15}N]Phe exists in two different conformations as seen by ^{13}C CPMAS. The resulting experimental ($\phi_{\text{Ala}}, \psi_{\text{Ala}}$) pair is ($+175^\circ, +120^\circ$) for conformation A and ($-170^\circ, +120^\circ$) for conformation B. The error estimations are $\pm 15^\circ$ for ϕ_{Ala} and $\pm 20^\circ$ for ψ_{Ala} . The ψ data are well resolved for α -helix vs β -sheet structures for non-glycine residues. In this new approach for determining conformational angles by MAS PM5-REDOR the analysis is simple and the technique can cope with the presence of two populations of conformations.

Acknowledgment. This work was supported by a grant from the Israeli Science Foundation. I.S. was supported with grants from the German Academic Exchange Service (DAAD) and the MINERVA-Foundation. We thank Jacob Anglister for help with ϕ and ψ angle conventions.

Supporting Information Available: PM5-REDOR plots (PDF). This material is available free of charge via the Internet at <http://pubs.acs.org>.

JA000489W

(58) Muchmore, D. C.; McIntosh, L. P.; Russell, C. B.; Anderson, D. E.; Dahlquist, F. W. *Methods Enzymol.* **1989**, *177*, 44–73.

(59) Hong, M.; Jakes, K. *J. Biomol. NMR* **1999**, *14*, 71–74.

(60) IUPAC–IUB Commission on Biochemical Nomenclature. *J. Biol. Chem.* **1970**, *245*, 6489–6497.